RESEARCH

Decellularization and enzymatic preconditioning of bovine uterus for improved recellularization

Edina Sehic[1,2], Lucía de Miguel-Gómez[1,2], Emy Thorén[1,2], Johan Sameus[1,2], Henrik Bäckdahl[3], Mihai Oltean[1,4], Mats Brännström[1,2,5] and Mats Hellström[1,2,3*]

Abstract

Background Uterus tissue engineering aims to repair a dysfunctional uterus that causes infertility, e.g., after significant scarring from benign or malign resection procedures. Decellularized uterine tissue provided regenerative support in several animal models as a biocompatible natural extracellular matrix (ECM) derived scaffold after uterine damage. However, variations in decellularization protocols and species used limit conclusive evidence and translational progress. Hence, a species-independent decellularization protocol could facilitate preclinical research. Therefore, we investigated if our developed sheep uterus decellularization protocol was species-independent and effective for the significantly larger bovine uterus. We further assessed if there were any negative post transplantation immunological consequences from the metalloproteinases 2 and 9 (MMP 2, MMP 9) treatment that was used as a preconditioning treatment to significantly improve scaffold recellularization after decellularization.

Methods Bovine uterus was decellularized using sodium deoxycholate, and the remaining ECM was quantitatively assessed for DNA, protein, and ECM components. The morphology and physical attributes were examined by immunohistochemistry, electron microscopy, and mechanical tests. Scaffold biocompatibility, bioactivity, and angiogenic properties were assessed with the chorioallantoic membrane assay (CAM) and the immune response following transplantation of MMP treated scaffolds was compared with untreated scaffolds in a rat model. The in vitro recellularization efficiency of the scaffolds was also assessed.

Results The decellularization protocol was effective for bovine uterus. The MMP treatment did not negatively affect scaffold immunogenicity in vivo, while the treatment potentiated mesenchymal stem cell recellularization in vitro. Furthermore, the decellularization protocol generated biocompatible and angiogenic uterine scaffolds.

Conclusion Bovine uterus was successfully decellularized using previously established protocols. These results confirm earlier findings in the sheep model and further indicate that MMP treatment may be beneficial. The results further conclude the development of a species-independent, reproducible, and biocompatible scaffold generation protocol that can provide an important element for successful translational research.

Keywords Uterus, Bioengineering, Decellularization, Metalloproteinases, Immune reaction

*Correspondence:
Mats Hellström
mats.hellstrom@gu.se
Full list of author information is available at the end of the article

Background

Scarring after resection procedures on the uterus, or from repeated cesarean sections cause significant tissue damage that negatively affect fertility and increases the risk of uterine rupture during a future pregnancy. Consequently, uterine rupture in a non-scarred uterus is rare (0.01%), while the risk increases 2.7-fold after just one cesarean section [12]. Furthermore, the risk after laparoscopic myomectomy or adenomyomectomy is substantial (1% and 8.7%, respectively) [43]. To prevent such serious adverse events, a grafted bioengineered uterine patch may be used to stimulate a scar-free tissue regeneration after surgery by covering the incision area at the end of each procedure, or a bioengineered uterine patch might be used to replace scarred tissue. A long-term goal may also include using a bioengineered uterus as a donor material in a uterus transplantation setting to bypass hurdles such as organ shortage, risky live donor surgery, and adverse immune suppression side-effects [36].

In the last decade, several proof-of-concept studies have reported restoration of fertility after transplantation of a bioengineered uterus patch in the mouse, rat, and rabbit [3, 13, 15, 16, 20, 23, 25, 28, 35, 42]. A successful approach to create a uterus scaffold is through decellularization. Most allogeneic donor cell components are removed in this process while a 3-dimensional extracellular matrix (ECM) with intact vascular conduits is preserved [13, 25, 35]. To date, successful uterus decellularization protocols have also been optimized for larger animals such as the pig [4] and the sheep [9, 39]. The sheep model played a significant role in preparing for the first successful human uterus transplantation trial at our center [2, 7] and is considered the best non-primate animal model for team-training before human uterus transplantation due its close similarity to the human uterus in terms of size, vascular anatomy, and pregnancy characteristics.

Variations in decellularization protocols between research groups and animal models hamper decisive conclusions and translational progress. More specifically, the rat uterus decellularization protocol published by our group in 2014 was not optimal for the much larger sheep uterus. Hence, new protocols were developed for the sheep uterus and the developed uterus scaffolds showed to be bioactive and stimulate angiogenesis and growth of neurites [9, 13, 31, 39]. Similarly, the first vascular perfusion decellularization study conducted on human uterus reported that a four-times longer decellularization process (38 days) was required compared with the sheep uterus (9 days), even when a high concentration of sodium dodecyl sulfate (SDS; 2%) was used [8]. Furthermore, different detergent protocols can affect the quality of the resulting scaffold, e.g., influencing the immunogenicity, recellularization efficiency, and the resulting fertility outcomes after transplantation [15, 29, 30]. Hence, further evaluation of less aggressive decellularization methods for large animal models, with a reproductive system that more closely resembles the human, is justified and the establishment of a species-independent uterus decellularization protocol would be advantageous to minimize further protocol development in future primate and human models to speed up translational research and simplify comparison between studies.

Hence, the main objective of this study was to evaluate whether our previously optimized sheep uterus decellularization protocol could be adopted for the much larger bovine uterus and evaluate its immunogenicity in a rat model.

Material & method

Uterus isolation, decellularization, and MMP preconditioning

In total, seven bovine uteri were isolated from cows at a local abattoir. Since animals were bred and processed for food production, no ethical approval was needed. Each uterus was dissected free from surrounding organs and tissue and the uterine arteries were canulated (20G, BD Neoflon, Becton. Dickinson GmbH, Heidelberg, Germany). The uterus was then flushed with ice-cold phosphate-buffered saline (PBS; Thermo Fisher Scientific, Gothenburg, Sweden) that included heparin (5000 IU/l; Leo Pharma, Ballerup, Denmark) and lidocaine (0.04 g/l; AstraZeneca, Gothenburg, Sweden). The perfused organ was then frozen (-20℃) in the same solution, and then processed by following our previously published sheep uterus decellularization protocol [39]. Briefly, each frozen uterus was thawed and perfused at room temperature with the first cycle of chemicals, including the ionic detergent sodium deoxycholate (SDC; 2%; Sigma Aldrich, Stockholm, Sweden), for eight hours (h), then with deionized water (DW) for 26 h, and PBS for 12 h. The organ was then perfused with Dulbecco's PBS (dPBS; 1 h, 37C°; Thermo Fisher Scientific, Stockholm, Sweden), and DNase I (1 h, 37C°; 8000UI per organ; Sigma Aldrich, Stockholm, Sweden), and then washed for 1 h with DW before repeating the same perfusion cycle a second time. After the second cycle, each uterus was sterilized by the perfusion of peracetic acid (0.1% in 0.9% NaCl) for 1 h and then washed by perfusing sterile PBS until a neutral pH was reached. The decellularized uterus was then cut into smaller tissue segments. Half the number of decellularized uterus pieces were further exposed to activated MMP 2 (2.5ug/L; Sigma-Aldrich, Stockholm, Sweden) and MMP 9 (2.5ug/L; Enzo Life Sciences, Farmindale, New York) at 37C° for 24 h [31], and then washed in a 20 mM EDTA solution (diluted in sterile PBS; two times

ten minutes) to increase the scaffold´s porosity and improve the downstream recellularization application of the scaffolds. Both scaffold types, the decellularized tissue (group DC), and the decellularized tissue with the additional MMP treatment (group DC^{MMP}) were frozen at -20 °C in sterile PBS until further analyzed.

DNA quantification, histology, and scanning *electron microscopy*

Tissue samples from native, decellularized uterus, and MMP-treated decellularized uterus were put on a filter paper to remove excess liquid and then weighed before homogenization (FastPrep-24 5G; MP Biomedicals, Irvine, USA). The tissue homogenate was centrifuged and further used for total DNA quantification using the DNeasy Blood and Tissue kit (#69,504; Qiagen, Sollentuna, Sweden) and a Nanodrop 2000 (Thermo Fisher Scientific).

Formalin-fixed scaffold biopsies were dehydrated and embedded in paraffin, and then sectioned at 5 μm on a microtome (HM355S; Thermo Fisher Scientific) and mounted on a glass slide. Histological analysis with 4′,6-diamidino-2-phenylindole (DAPI) staining and hematoxylin and eosin (H&E) was performed using standard protocols to investigate general morphology and the remaining DNA content after decellularization and MMP treatment. Standard staining protocols were also used for Masson's trichrome (MT; HT15-1KT; Sigma Aldrich, Stockholm, Sweden), Alcian Blue (AB; HL28014.0250; Histolab, Gothenburg, Sweden), and Verhof-van Gieson (VVG; ab150667, Abcam, Cambridge, UK) to visualize collagen, sulfated glycosaminoglycans (sGAGs), and elastin in native bovine uterus tissue, and in the two scaffold types. All slides were imaged using a microscope slide scanner (Axioscan 7; Carl Zeiss, Oberkochen, Germany).

Samples were also fixed for scanning electron microscopy following standard procedures at the center for cellular imaging (CCI), Sahlgrenska academy, university of Gothenburg. The thickness of 150 collagen fibers in the respective scaffold types was quantified from scanning electron microscopy images at 39.000×magnification from a total of three different images ($n=3$) using ImageJ.

Protein and ECM quantification

Tissue homogenate from native uterus and both scaffold types (DC and DC^{MMP}) was also processed for protein quantification using the bicinchoninic acid (BCA) protein extraction kit 2000 (#23,227; Thermo Fisher Scientific). The ECM composition was quantified using the colorimetric-based assays developed by Biocolor (Carrickfergus, UK) by following the manufacturer's instructions. More specifically, the soluble and insoluble collagen were assessed using Sircol™ S1000 and S2000, respectively. Elastin and sGAGs were quantified using Fastin™ F2000 and Blyscan™ B1000, respectively.

Mechanical tests

Ring biopsies, containing all uterine layers, from group DC ($n=21$) and group DC^{MMP} ($n=7$) were compared with native bovine uterus biopsies ($n=10$). The tensile testing was completed using the Zwick/Roell Z1.0 (Zwick, Ulm, Germany), which utilized a pre-load of 0.1 N and a test speed of 20 mm/min. The accuracy of the tester was 0.5% (force) and 0.5% (elongation) based on regular calibrations in accordance with ISO 7500–1 and ISO 9513. The maximum load, modulus, and work needed to completely deform the tissue rings were recorded and normalized to the measured sample width.

Scaffold biocompatibility and bioactivity assessment

The chick embryo chorioallantoic membrane (CAM) assay was performed by incubating fertilized chicken eggs to embryo development day (EED) 3 at 37.5°C. Then, using a sterile 25G needle and syringe, 3 mL albumin was removed from each egg to detach the CAM from the shell. A 1cm^2 window was then removed from each shell using a scalpel, and the opening was covered with Tegaderm™ film (3 M Health Care, Minneapolis, Minnesota, USA) before each egg was returned to the incubator. At EDD 9, a biopsy (5 mm in diameter) from each scaffold type (DC, $n=10$; DC^{MMP}, $n=7$) was placed on the CAM inside the egg. A control group was included in the experiment by placing an inert hydrogel drop on the CAM instead of a scaffold type ($n=5$; 2.2% alginate crosslinked with CaCl$_2$; 100 mmol/L in PBS, Thermo Fisher Scientific) to establish a reference point that allows the quantification of normal blood vessel growth. After the insertion of the biomaterial or the hydrogel drop, the shell opening was again covered with Tegaderm™ and the egg returned to the incubator. At EDD 14, blood vessel formation around the inserted biomaterial was photographed (iPhone 13, Apple Inc, Cupertino, CA, USA). From the photograph of each implant, two rings were digitally inserted in the picture at the biopsy center using ImageJ (0.5 mm-1.5 mm from the center). The number of vessels was then manually counted in the area between these rings (branching vessels were counted as one) by two independent observers, blinded to the experimental groups. An average for each egg was then calculated and used for the statistical analysis.

In vivo transplantation

To investigate if the MMP treatment was causing any additional negative immunological effects, tissue patches (10×5 mm) from both scaffold types were transplanted

Sehic *et al. Translational Medicine Communications* (2024) 9:16

Page 4 of 13

in a rat model. A total of 12 female Sprague Dawley rats (8–10 weeks old, 140-180 g; Charles River, Sulzfelt, Germany) were used for the study that had previously been evaluated and approved by the local animal welfare committee (document 22/586, Gothenburg, Sweden). Under isoflurane anesthesia (2.5%; Baxter, Deerfield, USA), six rats received a decellularized bovine uterus tissue patch under the skin. An additional six rats received a scaffold from the DC^{MMP} group. Each graft was fixed with a 6:0 prolene suture (Ethicon, Raritan, USA) to the underlying tissue. The skin was then closed with titanium clips (Reflex 7; AgnThos, Stockholm, Sweden). Each rat was administered post operative analgesics (carprofen, 5 mg/kg, Orion Pharma, Danderyd, Sweden; buprenorphine, 0.05 mg/kg, RB Pharmaceuticals) for two days. On day 14 post transplantation, the grafts were retrieved from the animal under deep isoflurane anesthesia. Each patch was then carefully isolated free from surrounding tissue and placed in 4% formaldehyde (Histolab) for 24 h and further processed for histological analysis.

Immunohistochemistry and leukocyte infiltration quantification

Immunohistochemistry was performed on sectioned biopsies from grafted tissue. Each section was exposed to an antigen-retrieval protocol (pressure cooked with citrate buffer; pH=6). Sections were then stained with primary antibodies (Abcam, Cambridge, UK) for CD45^{+} (leukocytes; ab10558; 1:800), CD4^{+} (T-cells; ab237722; 1:100), CD8^{+} (cytotoxic T-cells; ab33786; 1:1000), CD163^{+} (class M2 macrophage; ab182422; 1:200), CD68^{+} (pan macrophage; ab31630; 1:000) and CD86^{+} (class M2 macrophages; ab220188; 1:100) diluted in tris buffered saline (TBS) with 0.05% tween-20 (Thermo Fischer Scientific). Visualization of the primary antibodies was conducted using the biotin-free alkaline phosphatase Mach 3$^{™}$ and vulcan fast red chromogen kits (Biocare Medical, Pacheco, CA, USA) by following the manufactures instructions. All slides were then imaged using a microscope slide scanner (Axioscan 7; Carl Zeiss). Six random areas were selected at 400×magnification (0.05mm^2/field) from each stained slide and the total number of positively stained cells was counted manually by one person blinded to the study groups.

Bovine fetal stem cell isolation and characterization

Bovine fetal stem cells (BF-SCs) were isolated from the femurs of calf fetuses with an estimated gestational age of 8–10 weeks [19] collected at a local abattoir. Femurs were flushed with L-15 medium supplemented with Gibco$^{™}$ antibiotic–antimycotic (Thermo Fisher Scientific). Isolated cells were then cultured and expanded under standard cell culture conditions using the Gibco$^{™}$ products DMEM medium (GlutaMAX$^{™}$) supplemented with antibiotic–antimycotic (Anti-Anti) and 10% fetal bovine serum (Thermo Fisher Scientific). Cells from passage five were then seeded and cultured for 14 days in an 8-well chamber slide ($5×10^3$ cells per chamber). Cells were verified for multipotency according to previously established methods by using differentiation media for chondrocytes [38] and osteocytes [21] respectively. After differentiation, BF-SCs were fixed in 4% formaldehyde and stained with AB (HL28014.0250; Histolab) and alizarin red (#42,040; Thermo Fisher Scientific) using standard methods for evaluating chondrogenesis and osteogenesis, respectively.

In vitro recellularization

Biopsy discs (5 mm in diameter) from both scaffold types (DC and DC^{MMP}; $n=18$ per scaffold type) were injected with a total of $1×10^6$ undifferentiated BF-SCs per disc using a 30G needle with 10 repeated injections. The recellularized discs were then placed in transwell inserts (0.4 μm, Sarstedt, Nümbrecht, Germany) and incubated with the endometrial side upwards for three hours with the cell suspension used during the cell injections. The discs were then completely covered with medium and cultured under standard cell culturing conditions. Recellularized discs were then fixed in 4% formaldehyde after three days and 14 days of culture, respectively. The recellularization efficiency was assessed by staining paraffin sections from each recellularized scaffold with H&E and DAPI ($n=9$ per scaffold type and time point). All slides were imaged using a microscope slide scanner (Axioscan 7; Carl Zeiss). Twelve areas were randomly selected at 200×magnification (0.02 mm^2/field) from each stained slide and the total number of cells was quantified using ImageJ. Each calculation was presented as the average total number of cells per mm^2 for each experimental group.

Statistics

Normal data distribution was tested for all sample groups using the Shapiro–Wilk test in the GraphPad Prism 9 software (GraphPad, CA, USA). If more than two groups were compared, the one-way ANOVA with Tukey's corrections was used for parametric data and results presented in mean±standard error of mean (SEM). For non-parametric data, the Kruskal–Wallis test with Dunn's post-hoc test for multiple group comparison was used and results presented as median±standard deviation (SD). If only two groups were compared, the Welch's *t*-test was used for parametric data, and the Mann–Whitney *U*-test used for non-parametric data. Differences were considered significant when $p<0.05$.

Sehic *et al. Translational Medicine Communications*   (2024) 9:16

Page 5 of 13

Results

Macroscopic, microscopic, and histological observations of the produced scaffolds

After decellularization, macroscopic evaluation of the organs showed that each uterus was whiteish and had preserved shape and size after the procedure (Supplementary Fig. 1A-C). Effective removal of nuclear material was confirmed with DAPI staining (Fig. 1A-C) and DNA quantification. No positively stained cells were observed in the decellularized tissue, although small fragments of DAPI staining were still visible in some decellularized organs. Even less DAPI staining was visualized in scaffolds exposed to the additional MMP treatment. When quantified, the DNA level had significantly decreased by 98.7% after the decellularization compared with native tissue (native uterus, median value = 2866 ng DNA/mg tissue ± 1077 SD; DC median value = 36.75 DNA/mg tissue ± 46.11 SD, $p = 0.0161$). The DNA level was further reduced and equaled 99.1% in DC^{MMP} scaffolds (median value = 24.75 ng/mg ± 19.42 SD, $p = 0.0005$ vs. native tissue). There was no significant difference in the DNA levels between the two scaffold types.

Histological assessment with H&E staining further confirmed the removal of cellular components and showed retained ECM morphology (Fig. 1D-F). Masson's trichrome staining showed well-preserved evenly distributed collagen fibers (blue), but a reduction of stained keratin and muscle fibers (red) in both scaffold types compared with native bovine uterus (Fig. 1G-I). VVG-stained tissue showed reduced elastin fiber staining (brown) in both scaffold types (Fig. 1J-L; collagen stained red). Staining of sGAGs through AB staining showed that the morphological arrangement was preserved after the decellularization procedures. However, there was a reduced staining intensity in the scaffolds compared with native tissue (Fig. 1J-L). No obvious differences could be distinguished after the additional MMP treatment of the scaffolds in any of the stained sections.

Scanning electron microscopy revealed an ECM-rich ultrastructure with bundles of collagen fibers in both scaffold types. At high magnification, abundant collagen fibers organized in a porous network were visualized after decellularization, with an even more porous network in the DC^{MMP} scaffolds (Fig. 2A-F). The collagen fiber thickness showed no significant difference in the two scaffold types compared with native uterus tissue (Fig. 2G).

Quantification of protein and extracellular matrix components

The total protein concentration was reduced from 56.65 μg/mg tissue (± 4.62 SEM) in native bovine uterus tissue to 15.63 μg/mg tissue (± 2.52 SEM; $p = 0.001$) in DC tissue, which is equivalent to 28% of its original protein content (Fig. 3A). The additional MMP treatment reduced the protein content further in the scaffolds to a mean value of 10.41 μg/mg tissue (± 1.20 SEM; $p = 0.001$ vs. native uterus), representing 18% of its original content. Hence, the total protein content was significantly reduced during decellularization, but there was no statistical difference in the protein content following the additional MMP treatment of the scaffolds (Welch's T-test; $p > 0.05$).

The sGAGs content, which is important for cell signaling and tissue organization and homeostasis, was reduced during the scaffold production (Fig. 3B), from a median content of 0.229 μg/mg tissue (± 0.024 SD) in native bovine uterus, to a median value of 0.028 μg/mg tissue (± 0.023 SD) in the DC group, representing a reduction of 88% during the decellularization process ($p = 0.051$). The additional MMP treatment to the scaffolds resulted in a median sGAGs content of 0.017 μg/mg tissue (± 0.023 SD), representing a significant reduction of 93% compared with native bovine uterus tissue ($p = 0.002$). However, the difference in sGAGs content between the DC group and the DC^{MMP} group was not significant (Mann–Whitney U-test, $p > 0.05$).

Elastin levels, which are essential for tissue resilience and elasticity, were reduced by an average of 25% during the decellularization process, and by an average of 32% after the additional MMP-treatment. However, this reduction was not significant compared with native bovine uterus tissue (native bovine uterus mean value = 2.543 μg/mg tissue ± 0.202 SEM; DC group mean value = 1.898 μg/mg tissue ± 0.336 SEM; DC^{MMP} group mean value = 1.732 μg/mg ± 0.208 SEM; Fig. 3C).

The insoluble collagen concentration was preserved during the decellularization process (Fig. 3D; native tissue mean value = 2.010 μg/mg tissue ± 0.151 SEM; DC group mean value = 2.378 μg/mg tissue ± 0.370 SEM; DC^{MMP} group mean value = 1.679 μg/mg tissue ± 0.170 SEM). However, the soluble collagen levels were significantly reduced and contained 41% (DC group), and 36% (DC^{MMP} group) of its original content, respectively (Fig. 3E; native bovine uterus mean value = 0.824 μg/mg tissue ± 0.111 SEM; DC group mean value = 0.334 μg/mg tissue ± 0.042 SEM; $p = 0.001$ vs. native tissue; DC^{MMP} group mean value = 0.299 μg/mg tissue ± 0.089 SEM, $p = 0.001$ vs. native tissue). Nevertheless, the total collagen difference, with essential tissue structural and adhesive functions, was not significant between the groups (Fig. 3F) and when measured, the reduction only represented 4% of the original content after the decellularization, and 30% from its original content after the additional MMP treatment (native bovine uterus mean value = 2.834 μg/mg tissue ± 0.229 SEM; DC group
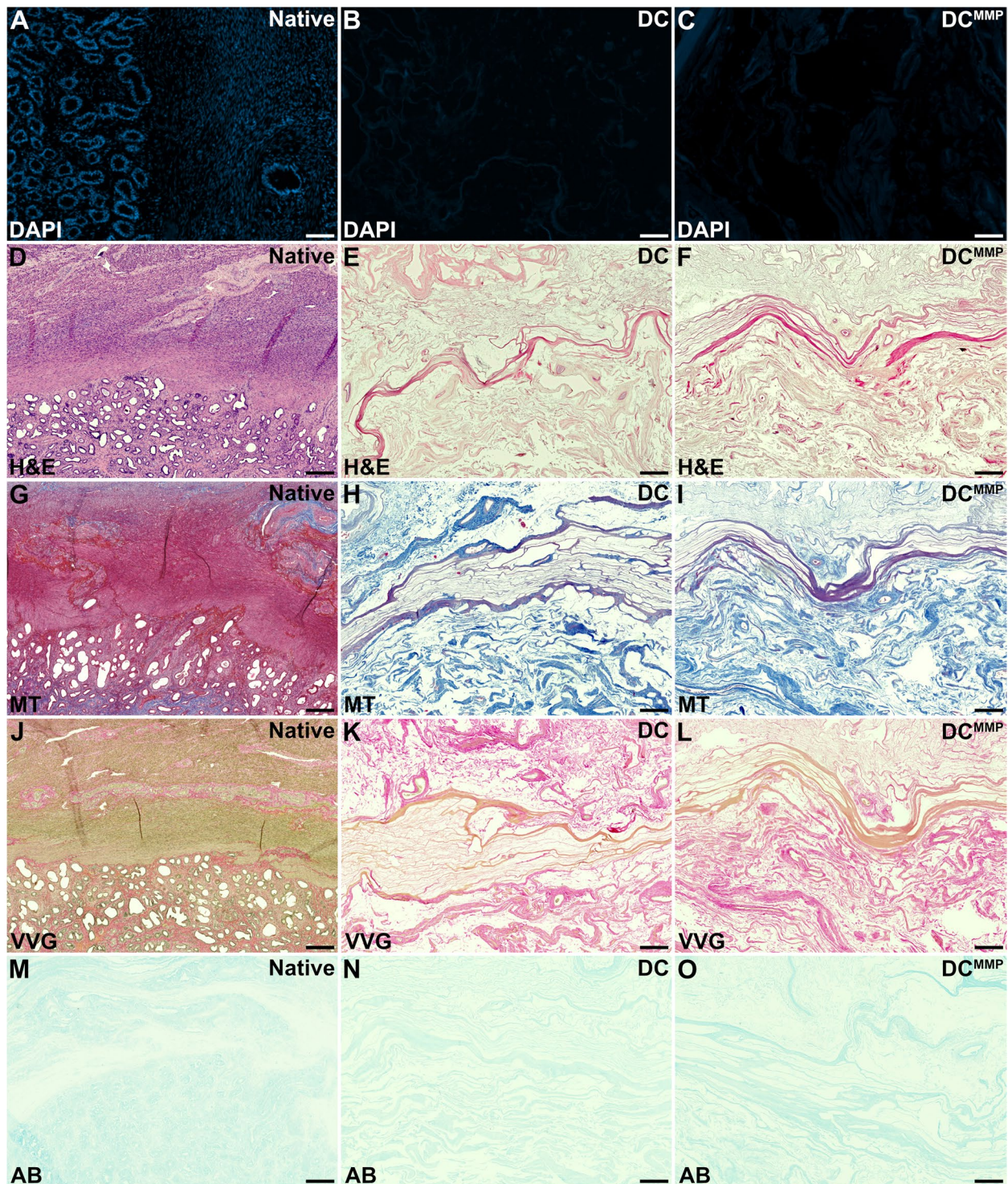
Fig. 1 Histological analyses of native bovine uterus, decellularized tissue scaffolds (DC), and MMP-treated scaffolds (DC^MMP). DAPI staining (**A**-**C**) confirmed the removal of DNA in all tissue layers. Hematoxylin and eosin stain (H&E; **D**-**F**) showed the removal of cells and remaining extracellular matrix morphology after the decellularization and subsequent matrix metalloproteinases treatment. Masson's Trichrome staining (MT; **G**-**I**) showed remaining collagen stained (blue) and keratin and muscle fibers (red). These components remained evenly distributed but showed a reduction in keratin and muscle fibers after decellularization. Similarly, Verhoeff-van Gieson stain (VVG; **J**-**L**) showed evenly distributed collagen fibers in the scaffolds (red), but a reduction in elastin fibers (brown). Alcian blue stain (AB; **M**–**O**) showed a remaining uniformed sulfated glycosaminoglycans composition after treatment in both groups. Scalebars; = 150μm
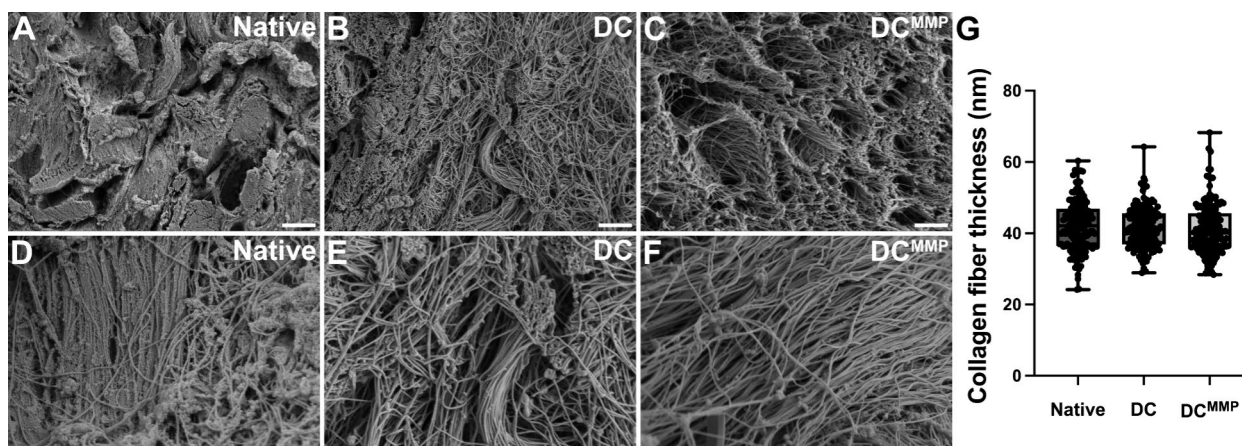
Fig. 2 Scanning electron microscopy analyses. Images of native bovine uterus, before (**A**, **D**) and after decellularization (DC; **B**, **E**) and subsequent matrix metalloproteinase treatment (DC.MMP; **C**, **F**). Imaging revealed a rich collagen fiber structure after decellularization and MMP treatment. Quantification of collagen fiber thickness (**G**) conducted in all groups showed that there was no significant difference between the groups. Scalebars; (**A**-**C**; magnification = ×15,500; scalebar = 2 µm); (**D**-**F**; magnification = ×40.000; scalebar = 750 nm)

mean value = 2.711 µg/mg tissue ± 0.380 SEM; DC^{MMP} group mean value = 1.979 µg/mg tissue ± 0.167 SEM), and there was no significant change following the additional MMP treatment.

Mechanical tests

In general, the decellularization process weakened the tissue and less force was required to tear the samples to a complete breaking point (Fig. 3G-I). This difference compared with native tissue reached significance for group DC on the maximum load required ($p = 0.026$; Fig. 3G), and for both scaffold types when the total work (J) required was assessed (Fig. 3H; DC vs. native tissue, $p = 0.0005$; DC^{MMP} vs. native tissue, $p = 0.008$). There was no significant differences when the more resistant structural components (i.e., collagen) were compared (modulus; Fig. 3I). The additional enzymatic treatment in group DC^{MMP} did not change the mechanical tests results compared with the DC group in any of the measurements.

Scaffold cytotoxicity and angiogenic bioactivity

Based on the CAM assay, there was an increased blood vessel growth around the biomaterials when the mean values were compared to the inert alginate control group (Fig. 4; mean normal blood vessel growth = 9.8 ± 0.8 SEM; mean blood vessels attracted to group DC = 14.2 ± 1.3 SEM, $p = 0.238$ vs. control group; mean blood vessels attracted to group DC^{MMP} = 14.4 ± 1.6 SEM; $p = 0.180$ vs. control group). However, this difference failed to be significant due to a large intra-group variation (Fig. 4D).

### Additional MMP treatment did not affect scaffold immunogenicity in vivo

The additional MMP treatment of the scaffolds did not negatively affect the immunogenic properties of the scaffolds after transplantation in rats (Table 1; Fig. 5). The total mean values of infiltrated leukocytes (CD4$^+$ cells), T-cells (CD4$^+$), cytotoxic T-cells (CD8$^+$ cells), pan-macrophages (CD68$^+$ cells), class M1 macrophages class (CD86$^+$ cells) and M2 macrophages (CD163$^+$ cells) were similar between the groups.

Cell differentiation and recellularization in vitro

The heterogenous BF-SCs isolated from the bovine fetus were multipotent showed by their ability to differentiate to chondrocytes and osteocyte (Supplementary Fig. 2A-D). Recellularization experiments with these cells, despite being mainly distributed to the superficial layers and around the injection sites, indicated that there was a significantly higher cell density after 3 days in DC^{MMP} scaffolds (mean value in DC tissue = 225 cells/mm^2 ± 12.4 SEM; mean value in DC^{MMP} scaffolds = 397.9 cells/mm^2 ± 33.98 SEM, $p = 0.0007$). However, after 14 days of culture, the beneficial effect had stagnated (mean value in DC tissue = 216.7 cells/mm^2 ± 25.59 SEM; mean value in DC^{MMP} scaffolds = 254.2 cells/mm^2 ± 53.91 SEM, $p = 0.5220$) (Fig. 6A-C).

Discussion

Pioneering work on whole uterus decellularization procedures for bioengineering applications was initiated around the time our group introduced clinical uterus transplantation as the first infertility treatment
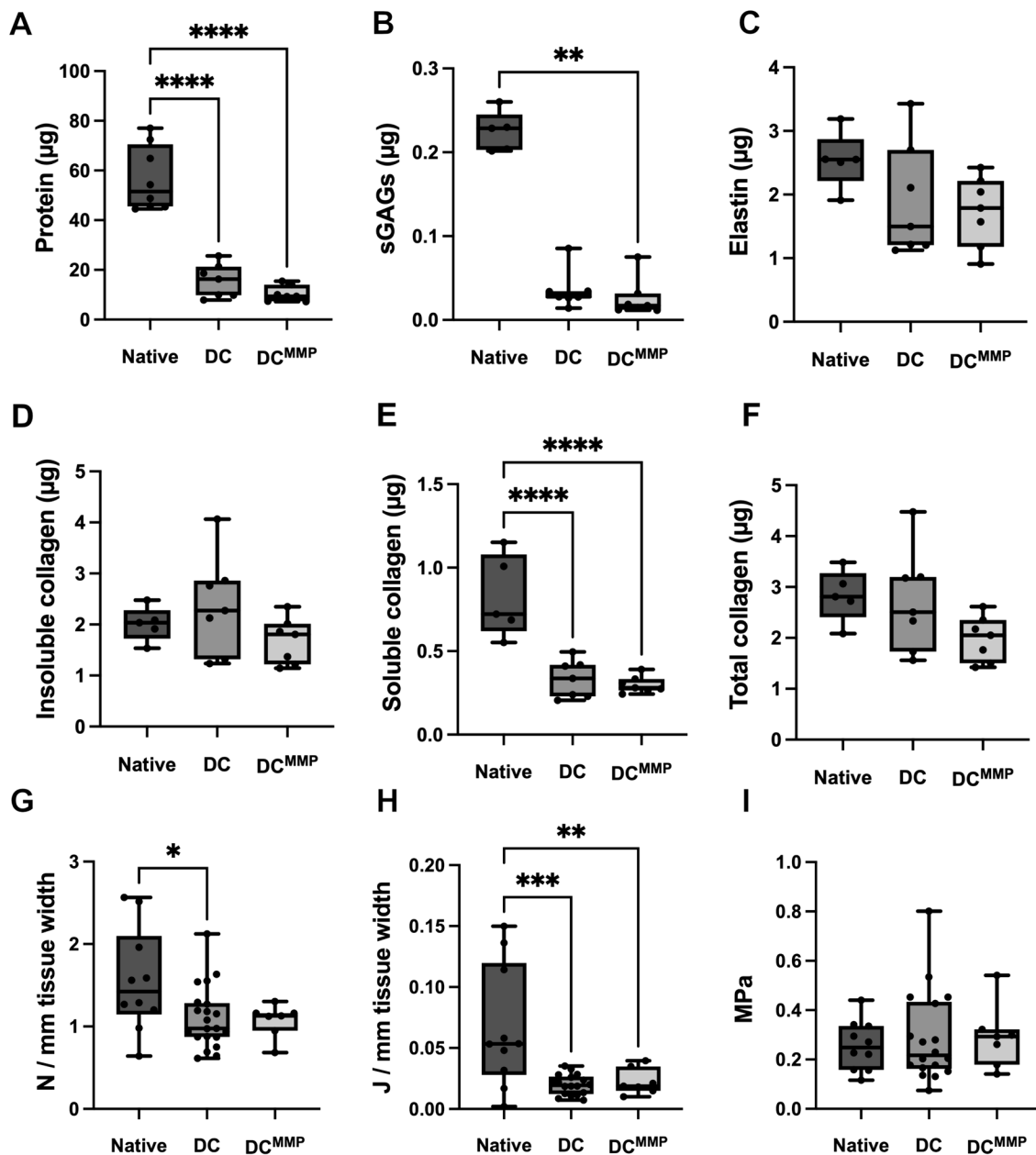
Fig. 3 Remaining extracellular matrix composition after decellularization and MMP treatment compared to native composition. Total protein (**A**), sulfated glycosaminoglycans (sGAGs: **B**), elastin (**C**), insoluble collagen (**D**), soluble collagen (**E**), and the total collagen (**F**) content per mg tissue after treatment is shown. The maximum load (**G**) and the work required to completely break the samples (**H**) were lower in the scaffolds than in native bovine uterus tissue. However, the load baring components within the tissue seemed less affected when the modulus was measured (**I**). Boxplot = median ± max–min. Significant levels = $* p < 0.05$; $* * p < 0.01$; $* * * p < 0.001$; $* * * * p < 0.0001$

for uterine factor infertility [14]. Since then, it has been evident that standardizing decellularization protocols for bioengineering applications is essential to expedite translational research to larger animal models, and to simplify comparison between studies [4, 8, 9, 13, 39]. We therefore tested our most promising SDC-based protocol developed for the sheep uterus on the larger

and readily accessible bovine uterus, before we plan to extend research to less accessible uterine material from non-human primates and humans. The bovine model does not completely reproduce the human reproductive system, but its bigger and thicker uterus was instrumental to elucidate the efficacy of our SDC-based protocol. We further evaluated the replicability
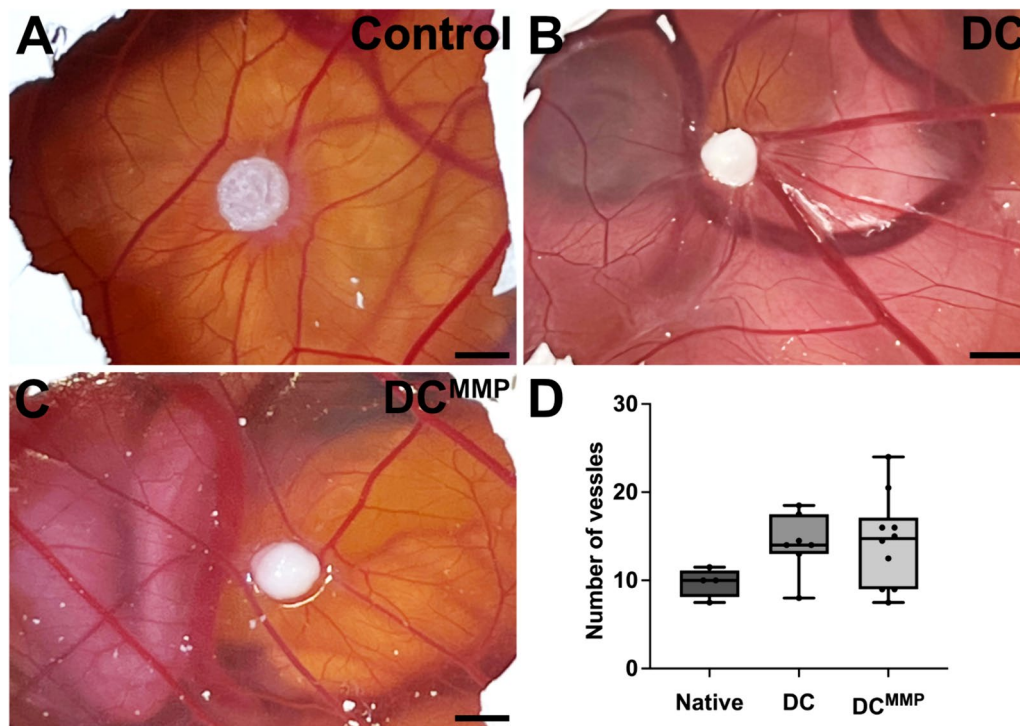
Fig. 4 Chorioallantioc membrane (CAM) assay for studying the scaffolds' biocompatibility and bioactivity. Angiogenesis was compared between an inert alginate control (**A**) and both DC (**B**) and DC^{MMP} (**C**) scaffolds by counting the number of blood vessels growing around them (**D**). Boxplot = median ± max–min; scalebars = 2 mm

Table 1 Leukocyte infiltration quantification. The total number of infiltrating immune cells/mm2 (CD45, CD4, CD8, CD68, CD163) was identified from cross-sections of subcutaneously transplanted material using antibodies and a MACH-3 polymer detection staining kit to identify positive cells. Data presented as mean number of infiltrating cells/mm2 ± SEM; $n = 6$ fields/animal. DC, decellularized tissue; DC^{MMP}, decellularized tissue with additional MMP treatment

| Cell type	DC	DC^{MMP}	P-value
Leukocytes (CD45 +)	1468 ± 85.81	1266 ± 129.3	0.2218
T-Cells (CD4 +)	587.2 ± 102.1	524.4 ± 53.67	0.5980
Cytotoxic T-cells (CD8 +)	329.5 ± 36.05	242.0 ± 48.87	0.1754
Pan-macrophages (CD68 +)	630.6 ± 114.5	576.1 ± 124.5	0.7543
M2-macrophages (CD163 +)	597.8 ± 74.21	428.9 ± 61.21	0.1097

of our advantageous MMPs preconditioning protocol that was shown to increase the recellularization efficiency in another species and confirmed that this enzymatic treatment did not have a negative impact on the recipient's immune response following transplantation. Importantly, we used a wide panel of tests to evaluate the tissue concerning its biochemical components, immunogenicity and ultrastructure and performed a detailed characterization of the decellularized bovine uterine tissue.

The current species divergence in efficacy of different decellularization protocols complicates the comparison between studies, significantly delaying translational research. For example, our initial studies on rat uterus decellularization showed that perfusion with dimethyl sulfoxide and Triton X-100 generated a scaffold type capable of restoring fertility in vivo [13, 15]. However, this protocol was inefficient when applied to the larger sheep model that required stronger detergents such as SDS or SDC [9, 39]. These protocol variabilities between species and the resulting divergences in scaffold composition have also been documented for other tissues, such as the lung [1] and aortic valves [41]. Similar protocol discrepancies were shown in the first human uterus perfusion decellularization protocol, which presented a fourfold longer process (38 days) than that required for the sheep uterus (9 days) [8]. Additionally, the quality of the resulting scaffold can be impacted by the selection of the detergent, as it may influence immunogenicity, recellularization efficiency, and fertility outcomes after engraftment [15, 29, 30]. Therefore, further evaluation of gentler decellularization methods for large animal models is necessary and the establishment of a standardized
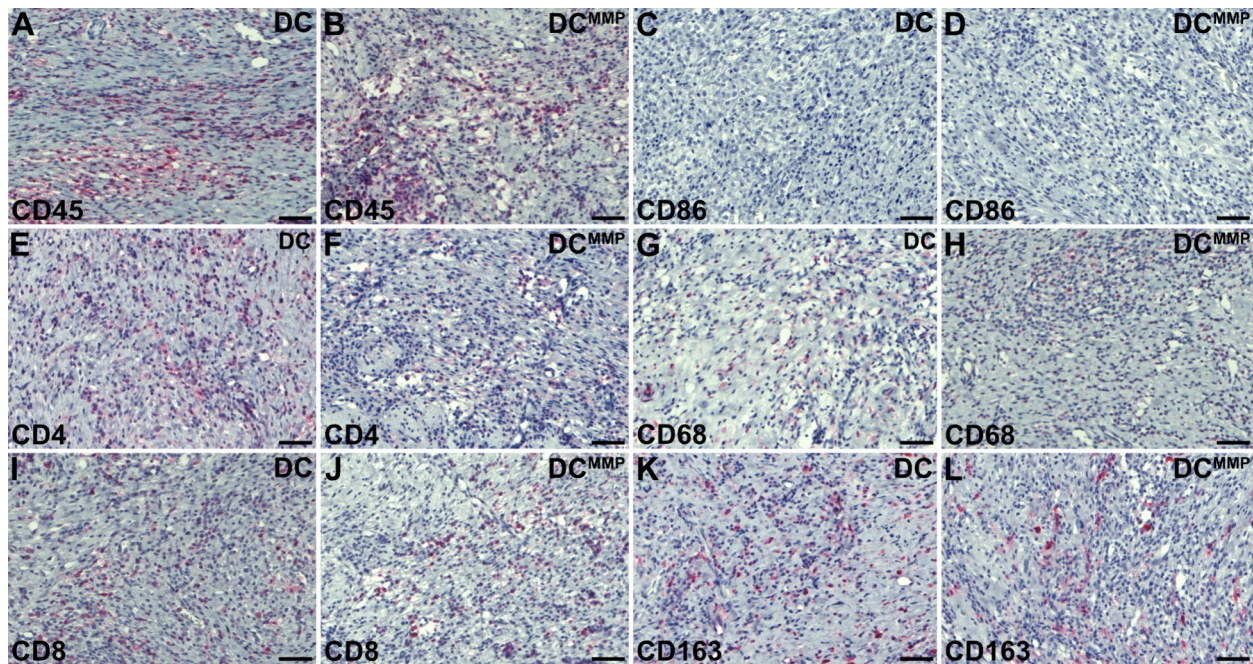
Fig. 5 Representative histological images of immune cell infiltration 14 days after subcutaneous transplantation. Positive cells were labeled red using MACH-3 staining detection kit for leukocytes (CD45; **A**-**B**), M1 macrophages (CD86; **C**-**D**), T-cells (CD4; **E**–**F**), macrophages (CD68; **G**-**H**), cytotoxic T-cells (CD8; **I**-**J**), M2 macrophages (CD163; **K**-**L**. The total number of positive cells from each field was quantified and presented as number of cells/mm^2; scale bars = 50 µm
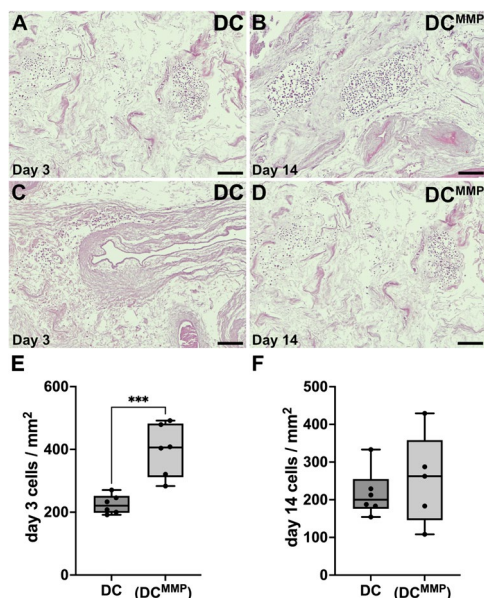
Fig. 6 In vitro recellularization. Scaffolds (DC and DC^{MMP}) were recellularized using bovine fetal bone marrow-derived stem cells and then in vitro cultured for 3 (**A** and **C**) and 14 (**B** and **D**) days. The recellularization efficiency was evaluated by counting the cells on the scaffolds after the two time points (**E** and **F**). Significant levels = ∗∗∗ $p < 0.001$; for exact p values, see the main text. Scale bars; 150 µm

species-independent uterus decellularization protocol will accelerate translational research and the initiation of novel clinical applications.

The results from the study presented herein confirm that our decellularization protocol for the sheep can also be applied for the bovine uterus. Histological and quantitative evaluations demonstrated preservation of important ECM structures and revealed no major difference after the additional MMPs treatment of the scaffolds. For example, there was a reduction of the soluble collagen following decellularization, but the total collagen amount remained similar, also for the DC^{MMP} group.

Further assessment using scanning electron microscopy showed a more porous tissue structure after decellularization, independent of the MMPs treatment, without any reduction in collagen thickness between groups (native, DC, and DC^{MMP}). Similar results have been observed by other research groups when decellularizing bovine intervertebral discs [18] or porcine uteri [4]. However, our previous work on the sheep uterus exhibited a significantly reduced collagen fiber thickness after decellularization and the MMP treatment [31]. Thus, it is still uncertain to what extent the observed differences in dimensions and structure of the ECM between the two species can be attributed to, e.g., native tissue density, given the generally lower average collagen thickness in

native bovine tissues compared with those on the sheep. For instance, Balestrini et al. documented a phylogenetic difference in ECM composition and properties (including collagen quantification) after decellularizing lungs from different mammals, including two non-human primate subspecies [1].

Mechanical tests on the scaffolds revealed a decrease in maximum load capacity and the required work for tissue deformation. This was expected since the decellularization process eliminates muscle fibers and other intra-cellular structural components, as reported in earlier uterus decellularization studies on e.g., the rat, sheep, pig, and human models [4, 8, 9, 13, 25, 39]. Interestingly, the modulus remained unchanged, aligning with the unchanged total collagen levels and fiber diameters. This suggests that important load-bearing components, such as collagen and elastin, were preserved since they are the first forces represented in the tensile test diagram [27].

We further assessed the functional bioactivity and cytotoxicity of our material with the well-established CAM assay [40], and confirmed that the MMPs treatment did not cause any further deleterious effects. There was also a tendency towards a higher level of blood vessels in the vicinity of the implanted biomaterials, indicating angiogenic scaffold properties, confirming earlier findings seen using the sheep model [31]. Nevertheless, the experiment confirms that the materials were biocompatible in a highly sensitive experimental model, and that the MMPs treatment did not negatively affect the scaffold's bioactivity.

Rejection of non-vascularized allografts develops slower than in vascularized allografts but occurs regularly within two weeks from transplantation [10, 33]. Therefore, we quantified the infiltration of six types of immune cells 14 days after engraftment and were able to confirm that the MMPs treatment did not negatively influence the immunogenicity of the scaffolds in vivo. This novel finding demonstrates that MMPs preconditioning is a safe improvement for preparing bioengineered bovine uterine tissue, despite that the innate immune response can be activated by damage-associated molecular patterns as a consequence of the decellularization process [11, 29, 30].

Lastly, it has been reported that the repopulation of decellularized uterus tissue leads to better regeneration of the target tissue in vivo [4, 5, 20], including improved immunotolerance when repopulated with stem cells [34, 37] or recipient-specific cells [26]. Regardless of discrepancies in, e.g., the cell source or applied recellularization method, surprisingly few groups quantitatively evaluated the in vitro recellularization efficiency in decellularized tissue. In the present study, we validated whether the MMPs treatment would improve the recellularization efficiency in the decellularized bovine uterus, as previously demonstrated in our sheep model [31], as it increases scaffold porosity and facilitates cell migration [22]. Indeed, our findings revealed a significant increase in cell density (76%) after 3 days culture in the MMP-treated scaffolds, but this beneficial effect halted after 14 days. These results contrasted with the previous sheep study, where the recellularization efficiency of MMP-treated tissue was further increased after 14 days. However, the differences in collagen fiber thickness and porosity between the two species may influence the process, as also discussed for other tissues [24]. Furthermore, recellularization is technically challenging and often results in individual variation, especially when using small biopsies. Nevertheless, improved recellularization strategies may include the use of Matrigel® to prevent detachment of added cells [32].

Even if our research focus is to translate uterus bioengineering protocols to human tissue, it would have been interesting to evaluate the possibility of xenograft scaffold transplantation. For example, the use of decellularized bovine pericardium and dermal matrix have been widely used in the clinic for carotid patch angioplasty [17] and abdominal wall reconstruction [6]. However, we did not investigate the xenograft compatibility of our material in a uterus repair model. Our small sample size, variations in age and hormonal cycle of the animals which the organs were collected from are additional limitations of our study. Consequently, slight differences in the uterine structure between specimen could be present and may have caused some of the intra group variability seen in the results.

Conclusion

A previously developed sheep uterus decellularization protocol was successfully applied to bovine uteri. This also suggest that the protocol should be advantageous in future expansion to non-human primate and human uterus decellularization. This would accelerate the translational approach towards clinical experimental studies in the human. Additionally, MMPs-treatment did not detrimentally affect scaffold composition or its immune reactivity in vivo providing additional evidence for its rational utilization for ECM derived scaffold recellularization.

Abbreviations

AB	Alcian blue
BCA	Bicinconinic acid
BF-SCs	Bovine fetal stem cells
CAM	Chorioallantoic membrane assay
CCI	Center for Cellular Imaging
DAPI	4',6-Diamidino-2-phenylindole
DC	Decellularized tissue
dPBS	Dulbecco's PBS
DW	Deionized water
ECM	Extracellular matrix
EED	Embryo development day

Sehic *et al. Translational Medicine Communications*　　　(2024) 9:16

Page 12 of 13

H&E	Hematoxylin and eosin
MMP 2	Matrix metalloproteinase 2
MMP 9	Matrix metalloproteinase 9
MT	Masson's trichrome
PBS	Phosphate-buffered saline
SDC	Sodium deoxycholate
SDS	Sodium dodecyl sulfate
SEM	Standard error of mean
sGAGs	Sulfated glycosaminoglycans
TBS	Tris buffered saline
VVG	Verhof-van Gieson

Supplementary Information

The online version contains supplementary material available at https://doi.org/10.1186/s41231-024-00175-x.

Supplementary Material 1: Supplementary Figure 1. Perfusion system and equipment used for decellularization of the bovine uterus. The custom perfusion system (A) consists of a perfusion pump and container where chemicals are perfused through the cannulated uterine arteries. Bovine uterus before (B) and after decellularization (C) using a sodium deoxycholate-based protocol. Scale bars = 2 cm.

Supplementary Material 2: Supplementary Figure 2. Differentiation of heterogeneous fetal bovine stem cells isolated from femurs of a bovine fetus. The isolated cells were expanded in vitro (A) and tested for pluripotency after stimulation and differentiation in vitro into chondrogenic lineage (alcian blue positive; B) and osteogenic lineage (alizarin red positive; C). Scale bars = 130 μm.

Declarations
The authors have nothing to declare.

Authors' contributions
Conceptualization, ES, MH, and MB; methodology, ES, ET, and JS; formal analysis, ES and MH; data curation, ES, LM-G, HB and MH; writing—original draft preparation, ES; writing—review and editing, LM-G, MO, MB and MH; supervision, MB and MH; project administration, MB and MH. All authors read and approved the final manuscript.

Availability of data and materials
All data generated or analyzed during this study are included in this published article.

Declarations

Ethics approval and consent to participate
The transplantation study had previously been evaluated and approved by the local animal welfare committee (Gothenburg, Sweden).

Consent for publication
Not applicable.

Competing interests
The authors declare no competing interests.

Author details
[1]Laboratory for Transplantation and Regenerative Medicine, Sahlgrenska Academy, University of Gothenburg, Gothenburg 405 30, Sweden. [2]Department of Obstetrics and Gynecology, Clinical Sciences, Sahlgrenska Academy, University of Gothenburg, Gothenburg 405 30, Sweden. [3]Unit of Biological Function, Division Materials and Production, RISE - Research Institutes of Sweden, Borås, Box 857, 50115, Sweden. [4]Department of Surgery, Clinical Sciences, Sahlgrenska Academy, University of Gothenburg, Gothenburg 405 30, Sweden. [5]Stockholm IVF-EUGIN, Hammarby Allé 93, Stockholm 120 63, Sweden.

References
1. Balestrini JL, Gard AL, Gerhold KA, Wilcox EC, Liu A, Schwan J, Le AV, Baevova P, Dimitrievska S, Zhao L, Sundaram S, Sun H, Rittié L, Dyal R, Broekelmann TJ, Mecham RP, Schwartz MA, Niklason LE, White ES. Comparative biology of decellularized lung matrix: Implications of species mismatch in regenerative medicine. Biomaterials. 2016;102:220–30.
2. Brannstrom M, Bokstrom H, Dahm-Kahler P, Diaz-Garcia C, Ekberg J, Enskog A, Hagberg H, Johannesson L, Kvarnstrom N, Molne J, Olausson M, Olofsson JI, Rodriguez-Wallberg K. One uterus bridging three generations: first live birth after mother-to-daughter uterus transplantation. Fertil Steril. 2016;106:261–6.
3. Campbell GR, Turnbull G, Xiang L, Haines M, Armstrong S, Rolfe BE, Campbell, JH. The peritoneal cavity as a bioreactor for tissue engineering visceral organs: bladder, uterus and vas deferens. J Tissue Eng Regen Med. 2008;2:50–60.
4. Campo H, Baptista PM, López-Pérez N, Faus A, Cervelló I, Simón C. De- and recellularization of the pig uterus: a bioengineering pilot study†. Biol Reprod. 2017;96:34–45.
5. Charoensombut N, Kawabata K, Kim J, Chang M, Kimura T, Kishida A, Ushida T, Furukawa KS. Internal radial perfusion bioreactor promotes decellularization and recellularization of rat uterine tissue. J Biosci Bioeng. 2022;133:83–8.
6. Clemens MW, Selber JC, Liu J, Adelman DM, Baumann DP, Garvey PB, Butler CE. Bovine versus porcine acellular dermal matrix for complex abdominal wall reconstruction. Plast Reconstr Surg. 2013;131:71–9.
7. Dahm-Kahler P, Wranning C, Lundmark C, Enskog A, Molne J, Marcickiewicz J, El-Akouri, RR, Mccracken, J & Brannstrom, M. Transplantation of the uterus in sheep: methodology and early reperfusion events. J Obstet Gynaecol Res. 2008;34:784–93.
8. Daryabari SS, Fendereski K, Ghorbani F, DehnaVI M, Shafikhani Y, Omranipour A, Zeraatian-Nejad Davani S, Majidi Zolbin M, Tavangar SM, Kajbafzadeh AM. Whole-organ decellularization of the human uterus and in vivo application of the bio-scaffolds in animal models. J Assist Reprod Genet. 2022;39:1237–47.
9. Daryabari SS, Kajbafzadeh AM, Fendereski K, Ghorbani F, DEhnavi, M, Rostami, M, Garajegayeh, BA & Tavangar, SM. Development of an efficient perfusion-based protocol for whole-organ decellularization of the ovine uterus as a human-sized model and in vivo application of the bioscaffolds. J Assist Reprod Genet. 2019;36:1211–23.
10. Djamali A, Odorico JS. Fas-mediated cytotoxicity is not required for rejection of murine nonvascularized heterotopic cardiac allografts. Transplantation. 1998;66:1793–801.
11. Gong T, Liu L, Jiang W, Zhou R. DAMP-sensing receptors in sterile inflammation and inflammatory diseases. Nat Rev Immunol. 2020;20:95–112.
12. Guise JM, Mcdonagh MS, Osterweil P, Nygren P, Chan BK, Helfand M. Systematic review of the incidence and consequences of uterine rupture in women with previous caesarean section. BMJ. 2004;329:19–25.
13. Hellstrom M, El-Akouri RR, Sihlbom C, Olsson BM, Lengqvist J, Backdahl H, Johansson BR, Olausson M, Sumitran-Holgersson S, Brannstrom M. Towards the development of a bioengineered uterus: comparison of different protocols for rat uterus decellularization. Acta Biomater. 2014;10:5034–42.
14. Hellström M, Bandstein S, Brännström M. Uterine Tissue Engineering and the Future of Uterus Transplantation. Ann Biomed Eng. 2017;45:1718–30.

15. Hellström M, Moreno-Moya JM, Bandstein S, Bom E, Akourl RR, Miyazaki K, Maruyama T, Brännström M. Bioengineered uterine tissue supports pregnancy in a rat model. Fertil Steril. 2016;106:487-496.e1.
16. Hiraoka T, Hirota Y, Saito-Fujita T, Matsuo M, Egashira M, Matsumoto L, Haraguchi H, Dey SK, Furukawa KS, Fujii T, Osuga Y. STAT3 accelerates uterine epithelial regeneration in a mouse model of decellularized uterine matrix transplantation. JCI Insight. 2016;1(8):e87591.
17. Ho KJ, Nguyen LL, Menard MT. Intermediate-term outcome of carotid endarterectomy with bovine pericardial patch closure compared with Dacron patch and primary closure. J Vasc Surg. 2012;55:708–14.
18. Illien-Jünger S, Sedaghatpour DD, Laudier DM, Hecht AC, Qureshi SA, IATRIDIS, J. C. Development of a bovine decellularized extracellular matrix-biomaterial for nucleus pulposus regeneration. J Orthop Res. 2016;34:876–88.
19. Krog CH, Agerholm JS, Nielsen SS. Fetal age assessment for Holstein cattle. PLoS ONE. 2018;13: e0207682.
20. Li X, Sun H, Lin N, Hou X, Wang J, Zhou B, Xu P, Xiao Z, Chen B, Dai J, Hu Y. Regeneration of uterine horns in rats by collagen scaffolds loaded with collagen-binding human basic fibroblast growth factor. Biomaterials. 2011;32:8172–81.
21. Liao HT, Chen CT. Osteogenic potential: Comparison between bone marrow and adipose-derived mesenchymal stem cells. World J Stem Cells. 2014;6:288–95.
22. Lozito TP, Jackson WM, Nesti LJ, Tuan RS. Human mesenchymal stem cells generate a distinct pericellular zone of MMP activities via binding of MMPs and secretion of high levels of TIMPs. Matrix Biol. 2014;34:132–43.
23. Magalhaes RS, Williams JK, Yoo KW, Yoo JJ, Atala A. A tissue-engineered uterus supports live births in rabbits. Nat Biotechnol. 2020;38:1280–7.
24. Malagón-Escandón A, Hautefeuille M, Jimenez-Díaz E, Arenas-Alatorre J, Saniger JM, Badillo-Ramírez I, Vazquez N, Piñón-Zarate G, Castell-Rodríguez A. Three-Dimensional Porous Scaffolds Derived from Bovine Cancellous Bone Matrix Promote Osteoinduction, Osteoconduction, and Osteogenesis. Polymers (Basel). 2021;3(24):4390.
25. Miyazaki K, Maruyama T. Partial regeneration and reconstruction of the rat uterus through recellularization of a decellularized uterine matrix. Biomaterials. 2014;35:8791–800.
26. Momtahan N, Sukavaneshvar S, Roeder BL, Cook AD. Strategies and processes to decellularize and recellularize hearts to generate functional organs and reduce the risk of thrombosis. Tissue Eng Part B Rev. 2015;21:115–32.
27. Muiznieks LD, Keeley FW. Molecular assembly and mechanical properties of the extracellular matrix: A fibrous protein perspective. Biochim Biophys Acta. 2013;1832:866–75.
28. Nie N, Gong L, Jiang D, Liu Y, Zhang J, Xu J, Yao X, Wu B, Li Y, Zou X. 3D bio-printed endometrial construct restores the full-thickness morphology and fertility of injured uterine endometrium. Acta Biomater. 2023;157:187–99.
29. Padma AM, Alshaikh AB, Song MJ, Akouri R, Oltean M, Brännström M, HELLSTRÖM, M. Decellularization protocol-dependent damage-associated molecular patterns in rat uterus scaffolds differentially affect the immune response after transplantation. J Tissue Eng Regen Med. 2021;15:674–85.
30. Padma, AM, Alsheikh, AB, Song, MJ, Akouri, R, Akyürek, LM, Oltean, M, Brännström, M & Hellström, M. 2021b. Immune response after allogeneic transplantation of decellularized uterine scaffolds in the rat. Biomed Mater, 16.
31. Padma AM, Carrière L, Krokström Karlsson F, SEHIC, E, Bandstein, S, Tiemann, TT, Oltean, M, Song, MJ, Brännström, M & Hellström, M. Towards a bioengineered uterus: bioactive sheep uterus scaffolds are effectively recellularized by enzymatic preconditioning. NPJ Regen Med. 2021;6:26.
32. Pors SE, Ramløse M, Nikiforov D, Lundsgaard K, Cheng J, Andersen CY, Kristensen SG. Initial steps in reconstruction of the human ovary: survival of pre-antral stage follicles in a decellularized human ovarian scaffold. Hum Reprod. 2019;34:1523–35.
33. Resende VC, Montero EF, Leão JQ, Manna MC, Koike MK, Pedrosa ME, SIMÕES MDE, J. Morphological changes on small-bowel fetal allografts in mice. Microsurgery. 2003;23:526–9.
34. Rodríguez-Fuentes DE, Fernández-Garza LE, Samia-Meza JA, Barrera-Barrera SA, Caplan AI, Barrera-Saldaña HA. Mesenchymal Stem Cells Current Clinical Applications: A Systematic Review. Arch Med Res. 2021;52:93–101.
35. Santoso EG, Yoshida K, Hirota Y, Aizawa M, Yoshino O, Kishida A, Osuga Y, Saito S, Ushida T, Furukawa KS. Application of detergents or high hydrostatic pressure as decellularization processes in uterine tissues and their subsequent effects on in vivo uterine regeneration in murine models. PLoS ONE. 2014;9: e103201.
36. Sehic, E, Brännström, M & Hellström, M. 2022a. Progress in Preclinical Research on Uterus Bioengineering That Utilizes Scaffolds Derived from Decellularized Uterine Tissue. Biomed Mater Devices.
37. Sehic E, Thorén E, Gudmundsdottir I, Oltean M, Brännström M, Hellström M. Mesenchymal stem cells establish a pro-regenerative immune milieu after decellularized rat uterus tissue transplantation. J Tissue Eng. 2022;13:20417314221118856.
38. Solchaga LA, Penick KJ, Welter JF. Chondrogenic differentiation of bone marrow-derived mesenchymal stem cells: tips and tricks. Methods Mol Biol. 2011;698:253–78.
39. Tiemann TT, Padma AM, Sehic E, Bäckdahl H, Oltean M, Song MJ, Brännström M, Hellström M. Towards uterus tissue engineering: a comparative study of sheep uterus decellularisation. Mol Hum Reprod. 2020;26:167–78.
40. Vargas A, Zeisser-Labouèbe M, Lange N, Gurny R, Delie F. The chick embryo and its chorioallantoic membrane (CAM) for the in vivo evaluation of drug delivery systems. Adv Drug Deliv Rev. 2007;59:1162–76.
41. Vedepo MC, Buse EE, Quinn RW, Williams TD, Detamore MS, Hopkins RA, Converse GL. Species-specific effects of aortic valve decellularization. Acta Biomater. 2017;50:249–58.
42. Yao Q, Zheng YW, Lin HL, Lan QH, Huang ZW, Wang LF, Chen R, Xiao J, Kou L, Xu HL, Zhao YZ. Exploiting crosslinked decellularized matrix to achieve uterus regeneration and construction. Artif Cells Nanomed Biotechnol. 2020;48:218–29.
43. Yazawa H, Takiguchi K, Ito F, Fujimori K. Uterine rupture at 33rd week of gestation after laparoscopic myomectomy with signs of fetal distress. A case report and review of literature. Taiwan J Obstet Gynecol. 2018;57:304–10.

Publisher's Note